PV-PCM Integration in Glazed Buildings. Numerical Study Through MATLAB/TRNSYS Linked Model

Hagar Elarga – University of Padova – hagar.elarga@dii.unipd.it
Francesco Goia – Norwegian University of Science and Technology – francesco.goia@ntnu.no
Ernesto Benini – University of Padova – ernesto.benini@unipd.it

Abstract

The paper describes the implementation of a 1-dimensional transient model based on the enthalpy method to analyse the thermal behaviour of a Phase Change Material (PCM) layer integrated in a window. The model and algorithm have been validated by comparison with experimental data. The model has then been expanded to couple a PV layer with the PCM layer. The complete model is implemented in MATLAB and linked to TRNSYS in order to estimate the dynamic thermal energy demand of a building equipped with a double skin façade with a PV-PCM layer in a ventilated cavity.

A parametric study was carried out, investigating three different cavity ventilation strategies for two European cities (Venice and Helsinki). The results show that, when the PCM layer is coupled with the PV layer, in Venice the cooling energy demand is 60 % lower, while in Helsinki the heating demand during the winter season is 36 % lower.

1. Introduction

PV modules conversion efficiency depends on the temperature of the panel, and an increment in PV surface temperature reduces the solar to electrical energy conversion efficiency by 0.4–0.5 %/K (Batagiannis et al., 2001). Therefore, the thermal control of PV modules (Machniewicz et al., 2015) is an important aspect to ensure effective solar energy conversion. According to the literature, six basic techniques for PV thermal management are possible: natural or forced air circulation, hydraulic or thermoelectric cooling, heat pipes, and the implementation of PCM. As far as the latter strategy is concerned, quite a few studies have appeared in the literature. A numerical PV/PCM model was presented and validated through comparison with experiments for three different configurations. This model provided a detailed insight into the thermal performance of a solid–liquid transition PCM when employed in a PV.

Ciulla et al. (2012) presented a one-dimensional thermal analysis of an isothermal PV-PCM model by using an explicit finite-difference approach. The numerical model was validated against experimental data given by a test facility in Palermo, Italy. Then, it can be used to determine the thermal behaviour of a multilayer (opaque) wall where PCM is coupled with a PV module. A simplified thermal network model to build integrated photovoltaic with PCM (BIPV-PCM) was analysed by Aelenei et al. (2014), it was developed in MATLAB/SIMULINK and validated with experimental results during the heating period. The comparison showed a good agreement, with most discrepancies occurring when airflow begins to flow into the gap. The maximum electrical efficiency of the PV system reached 10 %. The economic consequences of applying PCM to a PV system in two different climates, were investigated by Hasan et al. (2014). They concluded that such a system is financially viable in higher temperature and higher solar radiation environments. The implementation of PCM in combination with PV seems a very promising technique but it requires a good design under many aspects (Machniewicz et al., 2015).

The aim of the study presented in this paper is to develop one-dimensional fixed nodal grid model for PV-PCM in double skin facades. The model is capable of describing, with a sufficient degree of accuracy, the optical and thermal performance of such a façade system, which is particularly

challenging in terms of modelling because of the cavity's airflow, and of the dynamic thermal and optical properties of the PCM.

The present work is a continuation of an activity presented by Elarga et al. (2016). It improves the simulation of the phase change of the PCM through the use of the enthalpy method, and couples the PV-PCM double skin façade to a building (modelled in TRNSYS) in order to calculate heating and cooling demands. The innovations presented in this paper are:

1. A validated one dimensional heat transfer model for the PCM layer based on the enthalpy linearization method; and
2. The coupling (co-simulation) of the PV-PCM double skin facade model, developed in MATLAB, with the model of a building in TRNSYS, in order to evaluate in detail the annual thermal energy demand of a building equipped with such a façade system.

A numerical study is also presented to highlight the importance of PCM cooling time related to external and internal building loads.

2. Methods

Different elements control the efficient implementation of the PCM in building components, especially the melting/solidification temperature range, specific heat capacity value, and the charging/discharging synchronization with thermal loads. Accordingly, accurate and effective modelling and simulation tools are required to ensure the proper selection of PCM type. Different methods have been proposed to track the phase transient behaviour of the material. In the present article, the numerical modelling is divided into three sections:

- Enthalpy method and validation.
- PV-PCM model implemented in MATLAB.
- MATLAB-TRNSYS coupling for annual simulations.

2.1 Enthalpy Method

The enthalpy method was proposed by Swaminathan and Voller (1992) in order to model the thermal

behaviour of the materials undergoing a phase change, under the assumption that a phase change occurs over an arbitrarily narrow temperature range. In this way, enthalpy can relate to the temperature by a piecewise continuous function. Enthalpy can be approximated with three temperature possibility ranges by assuming constant specific heat capacity in each phase, as in Equation 1.

$$H=\begin{cases} c_s T & T \leq T_{m-\epsilon} \\ c_s(T_m-\epsilon) + \left[\frac{c_s+c_l}{2} + \frac{L}{2\epsilon}\right](T - T_m+\epsilon) & T_{m+\epsilon} < T < T_{m-\epsilon} \\ c_l T + (c_s - c_l)T_m + L & T \geq T_{m+\epsilon} \end{cases} \quad (1)$$

where ϵ is an arbitrarily small value representing half the phase change temperature interval. The approximate definition H(t) can be differentiated into Equation 2 with respect to temperature:

$$C^A = \frac{dH}{dT} = \begin{cases} c_s & T \leq T_{m-\epsilon} \\ \left[\frac{c_s + c_l}{2} + \frac{L}{2\in}\right] & T_{m+\epsilon} < T < T_{m-\epsilon} \\ c_l & T \geq T_{m+\epsilon} \end{cases} \quad (2)$$

The definitions of H(T) and C^A can be used to linearize the discretized enthalpy equation in iterative form as in Equation 3:

$$\sum a_{nb} T_{nb} - (a_p + \rho C^A)T_p{}^n = a_p \rho C^A T_p{}^{n-1} - \rho \cdot \frac{v}{\Delta\tau}\left[H_P{}^\circ - H_P{}^{n-1}\right] \quad (3)$$

Where:

$H_P{}^\circ$: Enthalpy node value of the previous time step

$H_P{}^{n-1}$: Enthalpy node value of iteration n-1

a: Nodal coefficients

τ: Time Step

The solution domain is defined where the derived linear equations form a matrix system and is solved instantaneously by inverting the matrix to obtain the temperature values according to an iterative scheme.

At the start of the time step the initial iterative fields are set to the previous time step values. From the known temperature field and enthalpy at iteration *n-1* the temperature nodes are achieved. In order to ensure solution consistency, a correction and iterative loop has to be followed by saving the solution of the matrix in the previous iteration, and

then re-solving the system after having corrected the nodal temperature T_p^n by Equation 4 with three possibilities of enthalpy ranges until convergence is reached. The code thus saves the calculated temperature field, and starts a new time step.

$$T_p^n =
\begin{cases}
\dfrac{H_P^n}{c_s}; & H_P^n \le c_s(T_m - \epsilon) \\[2ex]
\dfrac{H_P^n + \left[\dfrac{c_s + c_l}{2} + \dfrac{L}{2\,\epsilon}\right](T_m - \epsilon)}{\dfrac{c_s + c_l}{2} + \dfrac{L}{2\,\epsilon}} & \begin{aligned} &H_P^n > c_s(T_m - \epsilon) \\ &H_P^n < c_l(T_m + \epsilon) + L \end{aligned} \\[3ex]
\dfrac{H_P^n - (c_s - c_l)T_m - L}{c_l}; & H_P^n \ge c_l(T_m + \epsilon) + L
\end{cases} \quad (4)$$

2.1.1 Mathematical model description

A nodal scheme was developed to describe the double glazed layered window integrated with PCM (Goia et al., 2012; Elarga et al., 2016). The PCM window is schematized in nine-temperature nodes (Fig. 1-a) and the code solves instantaneously the nine linear equations. The validation of the model was carried out by comparing the numerical simulations with the data measured by Goia et al. (2015). For the sake of brevity, only half of the RC model is illustrated in Fig. 1-b since the scheme is symmetric.
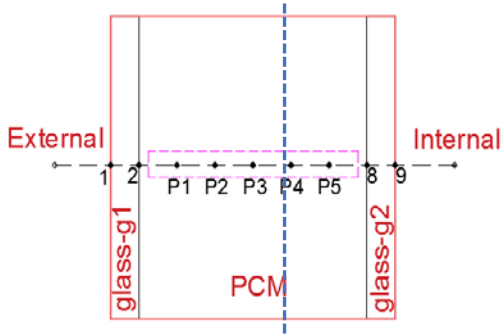
(a)
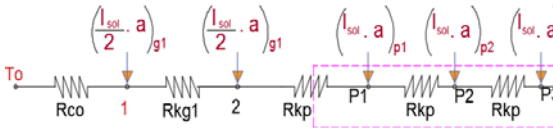
(b)

Fig. 1 – PCM glazing scheme (a), (b) symmetric scheme of RC model

Nodes (1) and (9):

$$\left(\frac{-k_{gl}}{x_{g1}} - h_o\right)T_1 + \left(\frac{k_{gl}}{x_{g1}}\right)T_2 = -I_s\left(\frac{a_{g1}}{2}\right) - (T_o h_o) \quad (5)$$

$$\left(\frac{k_{g2}}{x_{g2}}\right)T_8 + \left(-h_i - \frac{k_{g2}}{x_{g2}}\right)T_9 = -I_s\left(\frac{a_{g2}}{2}\right) - (T_i h_i) \quad (6)$$

Nodes (2) and (8):

$$\left(\frac{k_{g1}}{x_{g1}}\right)T_1 + \left(-\frac{k_{g1}}{x_{g1}} - \frac{k_{p1}}{x_{p1}}\right)T_2 + \left(\frac{k_{p1}}{x_p}\right)T_{p1} = \quad (7)$$
$$-I_s\left(\frac{a_{g1}}{2}\right)$$

$$\left(\frac{k_{g2}}{x_{g2}}\right)T_9 + \left(-\frac{k_{g2}}{x_{g2}} - \frac{k_{p5}}{x_{p5}}\right)T_8 + \left(\frac{k_{p5}}{x_p}\right)T_{p5} = \quad (8)$$
$$-I_s\left(\frac{a_{g2}}{2}\right)$$

PCM nodes (3:7); each homogenous sub-layer (from the five nodes comprising PCM layers) is represented by a conductive resistance and the enthalpy term. The resulting thermal balance Equation 9 is shown for one node only (P2).

$$\left(\frac{k_p}{x_p}\right)T_{p1} + \left(-2\frac{k_p}{x_p} - \frac{\left(\rho \cdot x_p \cdot (c^A)\right)_{p2}}{\Delta\tau}\right)T_{p2} +$$
$$\left(\frac{k_p}{x_p}\right)T_{p3} = -I_s \cdot \left(\frac{a_{p2}}{2}\right) +$$
$$\left(\frac{\left(\rho \cdot x_p \cdot (c^A)\right)_{p2}}{\Delta\tau}\right)^{n-1} T_{p2}^{\;n-1} - \rho\frac{x_p}{\Delta\tau}\left[H_P^{\circ} - H_P^{\;n-1}\right] \quad (9)$$

2.1.2 Short-wave radiation

Within the PCM layer, the analysis of the optical performance, and accordingly the short wave radiation, is not simple because the PCM has variable optical characteristics that depend on the current physical status of the material. When the PCM is in solid state, the dominant transmission mode is (direct to diffuse), and the scattering effect is prominent. While in the liquid phase the transparency increases and (direct to direct) transmission takes place. Accordingly, the optical properties such as absorption, scattering, and transmission, which control the radiation propagation within the PCM, were evaluated based on auxiliary equations that compute the nodal optical properties as a function in the liquid fraction β. The

liquid fraction value is the relative amount of liquid phase present in the PCM. This approach has been explained thoroughly in Gowreesunkera et al. (2013) and Elarga et al. (2016). The code is then able to identify the solar radiation energy balance for each time step of the entire glazing-PCM assembly. The final resultant solar radiation transmitted to the façade cavity (i.e. the solar gain), is then provided to the TRNSYS model as input, as explained in Section (2.3), to calculate the hourly profile of the thermal loads.

2.1.3 Enthalpy linearization method validation

Experimental data available in the literature (Goia et al., 2012) for a PCM glazing made of two panels of clear glass and a layer of paraffin wax (15 mm thickness) was used for validation purpose. A comparison between the measured and calculated surface temperature values of the inner and outer glass layers as illustrated in Fig.s 2a and 2b respectively for a week during the summer, has shown a good agreement. The RMSE for the inner glass reached 1.6 °C and within the outer glass 2 °C.
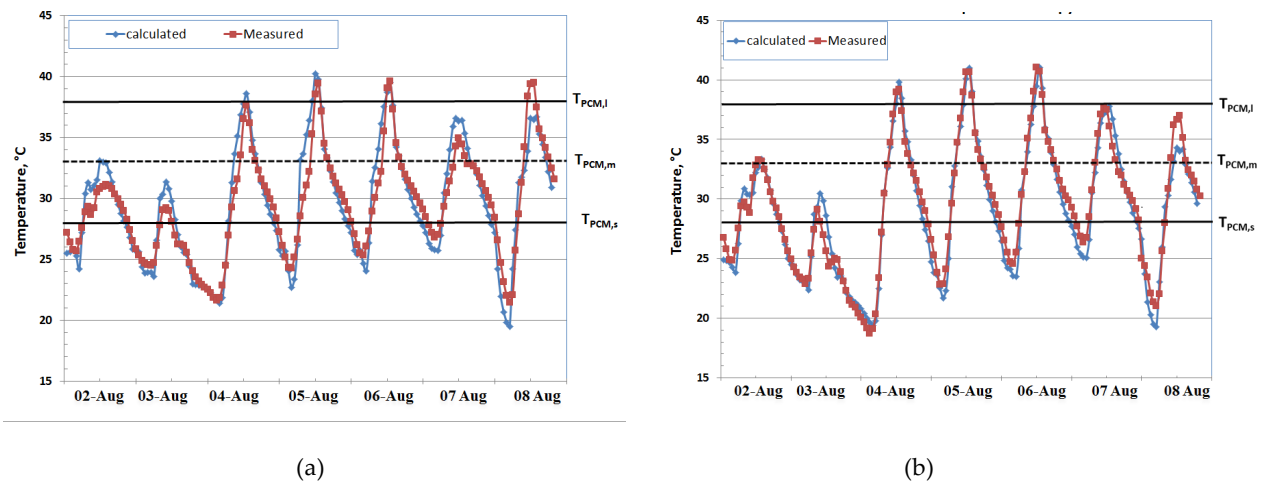

(a)   (b)

Fig. 2 – Numerical Model validation, calculated vs measured, (a) inner glass surface, (b) outer glass
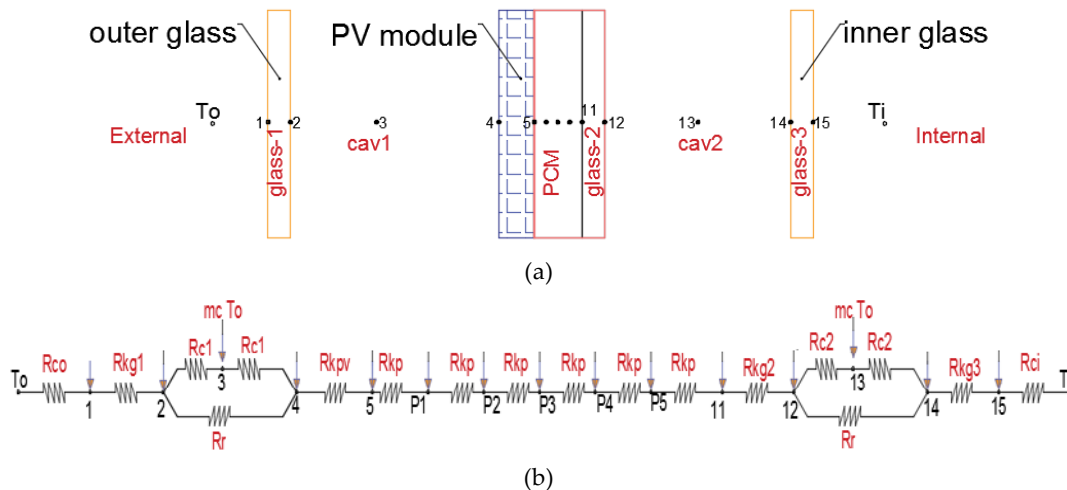

(a)

(b)

Fig. 3 – Numerical Model validation, calculated vs measured, (a) inner glass surface, (b) outer glass

2.2 PV-PCM Resistance Model in MATLAB

The second model developed is that of a PCM layer integrated with a PV module, and installed inside a façade cavity composed of two glass layers (the inner and outer) as shown in Fig. 3a. The entire 1-D numerical model of the glazed façade was developed. Thermal nodes of each element are illustrated in Fig. 3b. PCM were divided into 5 homogenous layers.

2.2.1 Mathematical model description

For the sake of brevity, the energy balance equations for Nodes 3 and 13 that describe the cavity ventilation from outside air (out-out technique), are presented below. The rest of the nodes are similar to Equations 5 to 9, previously mentioned. More information on this model can be found in Elarga et al. (2016).

$$(h_{c1})\, T_2 + (-2\, h_{c1} - m \cdot c)T_3 + (h_{c1})T_4 = -(m \cdot c)T_o \tag{10}$$

$$(h_{c2})\, T_{12} + (-2\, h_{c2} - m \cdot c)T_{13} + (h_{c2})T_{14} = -(m \cdot c)T_o \tag{11}$$

2.2.2 PCM Technical specifications

It is important to highlight that PCM physical specifications $(T_m, h_{PCM}, L, c_s,\ c_l)$ are those of a real, commercially available product (Rubitherm RT35), and summarised in Table 1.

Table 1 – PCM Table of properties

Name	RT35- Organic
Solid temperature	29°C
Nominal melt. temperature	33°C
Liquid temperature	36°C
Specific heat Capacity	2 kJ kg^{-1} K^{-1}
Latent heat of fusion	160 kJ kg^{-1}

2.3 MATLAB-TRNSYS Coupling

In order to obtain a reliable simulation of the impact of a PV-PCM double skin façade on the building energy demand it is necessary to link the previously presented PV-PCM 1-D model developed in MATLAB to TRNSYS (Klein et al., 2009). TRNSYS is a dynamic thermal model that takes into account the external, internal loads and the stored heat in the building components. The interaction between MATLAB and TRNSYS simulation studio was carried out using TYPE 155 from TRNSYS library. This type is dedicated to read external codes executed by MATLAB. The numerical algorithm starts by linking the required weather condition from TYPE 16 to both the MATLAB and the zone built in TRNbld (TYPE 56). Generally, it is mandatory to link the weather file to (TYPE 56) in order to operate the simulation model. On the other hand, for each listed inner zone on (TYPE 56), there is the availability to set its input data and boundary conditions as a user defined option. The PV-PCM - 1D numerical code estimates the temperature and transmitted solar radiation for each of the fixed grid nodes, including the last node that represents the inner surface layer temperature Node 15 (see Fig. 3a). However, the transient interface between TRNSYS and MATLAB models happens in air node B (see Fig. 4), i.e. Node 13 (Fig. 3a). The estimated transmitted solar radiation and air temperature with a five-minute time step are read as a user defined value for the inner layer zone on (TYPE 56). The reason behind considering the coincident interface between the two models in node B is that the complete room structure and the correspondent radiative/convective heat exchange (which include thermal storage of the room components) are computed by the MATLAB code alone. These heat transfer components have an influence on the energy balance of the inner glass layer and its final surface temperature. The inner glass layer was identified in the TRNbld (TYPE 56) library with the specifications as in Table 2. The considered facade is west oriented.

Table 2 – Glazed layer specifications

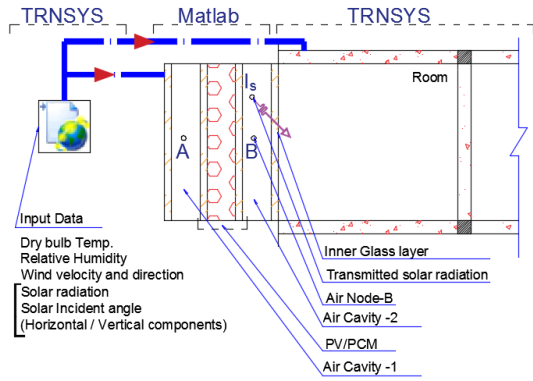| Density (kg/m³)	2500
Heat capacity kJ/(kg K)	0.84
Conductivity kJ/(h m K)	0.27

Fig. 4 – MATLAB/TRNSYS link scheme

2.4 PV.PCM Module Cavity Ventilation

The influence of the façade cavity ventilation schedule on the building energy performance is very relevant in general, and especially after PCM integration given the ventilation, strategy resides in controlling the pattern of phase changing. A compromise evaluation through three strategies was analysed, shown in Fig. 5. Strategy 1 assumed ventilation all year at day-time, Strategy 2 during the winter season the ventilation stopped entirely while in the summer season it was on during night hours, Strategy 3 assumed ventilation off all year. The ventilation volume flow rate was assumed 5 l/s per façade meter and the ventilation technique was (out-out), i.e. air flows from the outside passing through the cavity and then expelled from the top to the outside again.

(a) The ventilation system of the façade cavity was on all year during working hours only.
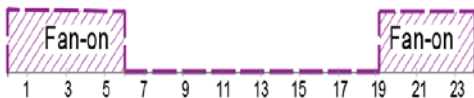
(b) This strategy investigates the ventilation influence throughout the summer season only during night hours from 8 pm to 7 am of the following morning.

(c) No active or passive ventilation system was considered in this strategy in order to investigate the PCM charge/discharge phase.

Fig. 5 – Different ventilation strategies during summer season, (a) Strategy 1, (b)-Strategy 2, (c)-Strategy 3

3. Results of the Parametric Analysis

The parametric study includes the comparison between the three ventilation strategies and a case of PV-PCM double skin façade, and a baseline case where the façade is without PCM. An open office area of 80 m² was considered in TRNbld (Klein et al., 2009) to estimate the yearly thermal loads. The internal loads were 70 W/person, 10 W/m² for lighting, and 130 W for the equipment. The following results were presented:

- Yearly thermal loads for each ventilation strategy and also a case study without the PCM (considered as a baseline reference).
- Inside operating temperature for each of the investigated cases (to highlight the PCM influence on the stability of the indoor temperature, and how that will support the peak load shaving).

3.1 Thermal Loads

Yearly thermal loads were calculated for two European cities with different climate classifications. Venice (Italy) with a fully humid, warm summer climate, and Helsinki (Finland) with a cool summer climate (Kottek et al., 2006). As shown in Fig. 6, the thermal performance varies according to the different investigated ventilation strategies. In Venice (Fig. 6a), during winter months, the highest consumption was recorded for Strategy 1 followed by the case without PCM. Strategies 2 and 3 came next with an almost similar pattern. The illustrated energy profiles were influenced by the PCM, and ventilating the cavity during daytime kept the PCM in its solid state. Under these conditions, the solar radiation transmission and the cavity temperature were reduced (Goia et al., 2015). Accordingly, the required thermal loads for Strategy 1 had the highest values. On the other extreme, the ventilation of the cavity during the night (Strategy 2) and the lack of ventilation (Strategy 3) allowed the PCM during daytime to be charged and melt, thus inducing a higher transmission and solar gains to the room. However, during the summer season, the highest energy consumption was recorded for the case without PCM (a predictable result), followed by Strategy 3 and finally, a similar pattern for Strategies 1 and 2.

In Strategy 3, the lack of cavity ventilation combined with higher solar radiation intensity and external temperature values caused the PCM to reach the melting phase without having a chance to be cooled and re-solidified (Turnpenny et al., 2000). Conversely, using the Strategies 1 and 2, ventilation allowed the PCM to be cooled either during the day or night-time to efficiently fulfill the purpose of integrating phase changing substances. In Helsinki (Fig. 6b), during summer season thermal energy demand (Strategy 3) with no ventilation shows the highest value compared to other cases, with the case without PCM being the next in line. Strategies 2 and 1 determine the minimum energy demand, with almost zero demand during all summer months in the latter strategy. This shows that a proper integration of PCM in building elements, combined with a right synchronization between PCM's charging/discharging phase and thermal loads can support the nearly zero energy-building concept (Zalba et al., 2004). During the winter season, the case without PCM and ventilation (Strategy 1) showed the highest energy demand, followed by Strategies 2 and 3, with the same thermal energy demand – as in both cases there was no ventilation of the cavity during the winter season.

3.2 Inner Zone Operating Temperatures

The impact of the PCM layer on the thermal comfort was investigated by analysing the inner zone operating temperatures for each strategy. In Fig. 7a; the daily profiles of the inner zone operating temperature are shown for July 16 (the design day for summer load). As shown, the closest profiles to the design temperature during working hours are those in case of ventilation (Strategies 1 and 2), followed by (Strategy 3) and the case without PCM. This can be explained by considering the PCM melting/solidification influence: the ventilation of the PCM during working hours or during the night improves the zone operating temperature and makes it closer to the desired setpoint temperature. Conversely, the lack of ventilation prevents the PCM from an efficient discharge phase, which leads to a performance similar to that of the reference case without PCM. In Helsinki, Fig. 7-b, the ventilation of the PV-PCM during working hours leads to indoor operating temperatures below the design set temperature by about 3 °C. Starting from midday, the difference decreased and the profiles were almost identical with the design temperature. This increment was due to the facade's west orientation and the solar intensity propagation. The temperature profiles for the (Strategy 3) and for the case without PCM were almost the same within the working hours. The difference reached 1.5 °C higher than the design set temperature.

(a)

(b)

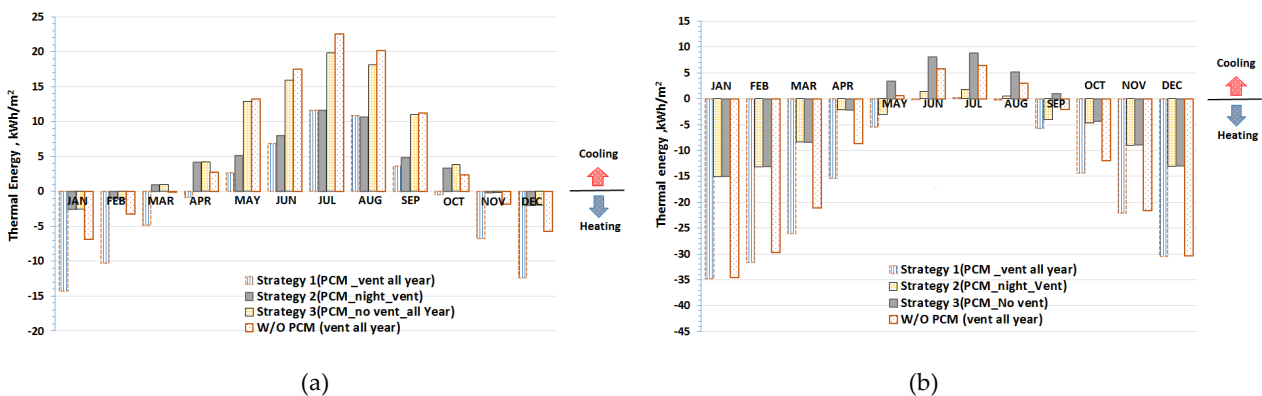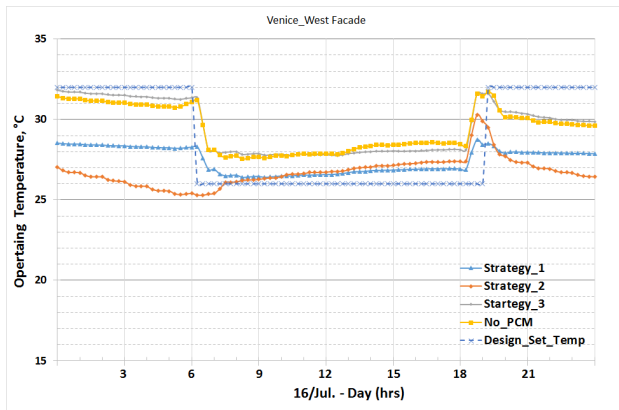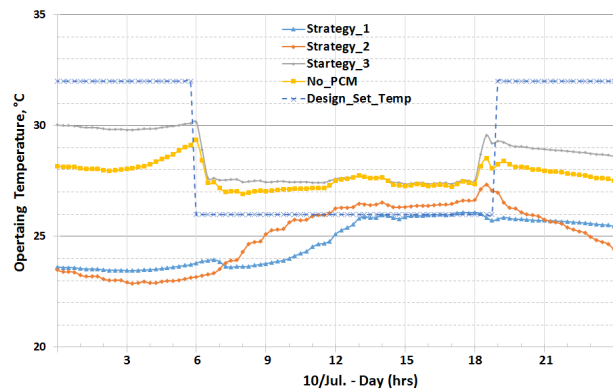Fig. 6 – Yearly thermal energy profiles, (a) Venice city, (b) Helsinki city

(a)   (b)

Fig.7 – Operating daily temperature profiles (a) Venice city, (b) Helsinki city

4. Conclusions

The article presents a validated numerical model that adopts the enthalpy method to describe a PCM glazing thermal performance. The model based on the enthalpy method was implemented in MATLAB to simulate an integrated PV-PCM system in a ventilated transparent façade. Then, this model was linked to an office building in TRNSYS environment, to estimate the dynamic thermal performance of the system (PV/PCM ventilated transparent façade and office building). Simulations were then carried out through a combination of software tools/models and the impact of three ventilation strategies on the performance of the system estimated for two European cities. The results show that the energy savings obtained through this façade system are significant and that PV-PCM can be a promising solution especially in Nordic countries, considering the thermal properties of the PCM as adopted in the simulation. In fact, it is important to stress that the PCM per-formance has to match transmission losses due to external temperature, solar radiation intensity, and internal loads, to be optimal. Further studies will focus on optimizing the features of the PCM in relation to different climates and ventilation strategies.

Acknowledgement

References

Aelenei, L., R. Pereira, H. Gonçalves, A. Athienitis. 2014. "Thermal Performance of a Hybrid BIPV-PCM: Modeling, Design and Experimental Investigation'". *Energy Procedia* 48: 474-483. doi:10.1016/j.egypro.2014.02.056.

Batagiannis, P., C. Gibbons. 2001. "Thermal assessment of silicon based composite materials used in photovoltaics." In: *Proceedings of Renewable Energy in Maritime Island Climates Conference*. Belfast, UK: UK-ISES.

Ciulla, G., V. L. Brano, M. Cellura, V. Franzitta, and D. Milone. 2012. "A finite difference model of a PV-PCM system." *Energy Procedia* 30: 198–206. doi:10.1016/j.egypro.2012.11.024.

Elarga, H., F. Goia, A. Zarrella, A.D. Monte, E. Benini. 2016. "Thermal and electrical performance of an integrated PV-PCM system in double skin façades: a numerical study". *Solar Energy* 136: 112–124. doi:10.1016/j.solener.2016.06.074.

Goia, F., M. Perino, M. Haase. 2012. "A numerical model to evaluate the thermal behavior of PCM

glazing system configurations". *Energy and Buildings* 54: 141–153. doi:10.1016/j.enbuild.2012.07.036.

Goia, F., M. Zinzi, E. Carnielo, V. Serra. 2015. "Spectral and angular solar properties of a PCM-filled double glazing unit". *Energy and Buildings* 87: 302–312. doi:10.1016/j.enbuild.2014.11.019.

Gowreesunkera, B.L., S. Stankovic, S. Tassou, P.A. Kyriacou. 2013. ''Experimental and numerical investigations of the optical and thermal aspects of a PCM-glazed unit''. *Energy and Buildings* 61: 239–249. doi:10.1016/j.enbuild.2013.02.032.

Hasan, A., S.J. McCormack, M.J. Huang, B. Norton. 2014. "Energy and Cost Saving of a Photovoltaic-Phase Change Materials (PV-PCM) System through Temperature Regulation and Performance Enhancement of Photovoltaics". *Energies* 7: 1318-1331. doi:10.3390/en7031318.

Klein, S., W. Beckman, J. Mitchell, J. Duffie, N. Duffie, T. Freeman. "TRNSYS 16 - A transient system simulation program, User manual". Madison, U.S.A.: University of Wisconsin-Madison.

Kottek, M., J. Grieser, C. Beck, B. Rudolf, F. Rubel. 2006. World Map of the Köppen-Geiger climate classification updated, *Meteorologische Zeitschrift* 15: 259-263. doi:10.1127/0941-2948/2006/0130.

Machniewicz, A., D. Knera, D. Heim. 2015. "Effect of Transition Temperature on Efficiency of PV/PCM Panels". *Energy Procedia* 78: 1684–1689. doi:10.1016/j.egypro.2015.11.257.

MATLAB 6.1, The MathWorks Inc., Natick, MA, 2000.

Rubitherm. 2016. HTTP://www.rubitherm.com. (Accessed: 12/2016).

Swaminathan, C.R., V.R. Voller. 1992. "A general enthalpy method for modeling solidification processes." *Metallurgical and Materials Transactions* 23: 651-664. doi:10.1007/BF02649725.

Turnpenny, J., D. Etheridge, D. Reay. 2000. "Noval ventilation cooling system for reducing air conditioning in buildings, Part I: Testing and theoretical modeling", *Applied Thermal Engineering* 20: 1019–1037. doi:10.1016/S1359-4311(99)00068-X.

Zalba, B., J. Marin, L. Cabeza, M. Harald. 2004. "Free cooling of buildings with phase change materials". *International Journal of Refrigeration* 27: 839–849. doi:10.1016/j.ijrefrig.2004.03.0.